IEEE Access
Multidisciplinary | Rapid Review | Open Access Journal

Received February 7, 2019, accepted February 22, 2019, date of publication March 5, 2019, date of current version March 25, 2019.

Digital Object Identifier 10.1109/ACCESS.2019.2902884

Construction of Rate-Compatible Raptor-Like Quasi-Cyclic LDPC Code With Edge Classification for IDMA Based Random Access

YUSHU ZHANG[1,2], KEWU PENG[1,2,3], (Senior Member, IEEE), ZHANGMEI CHEN[1,2], AND JIAN SONG[1,2,3], (Fellow, IEEE)

[1]Department of Electronic Engineering, Tsinghua University, Beijing 100084, China
[2]Beijing National Research Center for Information Science and Technology (BNRist), Research Institute of Information Technology, Tsinghua University, Beijing 100084, China
[3]Shenzhen City Key Laboratory of Digital TV System, Shenzhen 518057, China

Corresponding author: Kewu Peng (pengkewu@tsinghua.edu.cn)

This work was supported in part by the Science, Technology and Innovation Commission of Shenzhen Municipality under Grant JCYJ20160331171115521, and in part by the National Natural Science Foundation of China under Grant 61621091.

ABSTRACT Recently, rate-compatible raptor-like quasi-cyclic low-density parity-check (RL-QC-LDPC) codes, which are a typical class of multi-edge type LDPC codes with excellent performance and high flexibility, have been adopted in the technical specification of 5G new radio (5G-NR). In this paper, the rate-compatible RL-QC-LDPC coded interleave division multiple access (IDMA), or called the enhanced IDMA, is developed as non-orthogonal multiple access (NOMA)-based random access solution, and various spectral efficiencies can be flexibly supported thanks to the rate compatible capability. First, 5G-NR LDPC codes are directly incorporated into enhanced IDMA-based random access, which can support a wide range of user loads with relatively low system throughput. Second, to improve the supported user load and system throughput, an edge-classification-based extension (ECE) algorithm is proposed to construct rate-compatible RL-QC-LDPC codes toward enhanced IDMA while taking into consideration the novel structural features of 5G-NR LDPC codes. Based on the two proposed edge-classification methods, the ECE can efficiently reduce the search space of base matrices for each extension round and effectively maintain enough diversity in the selected seed base matrices to facilitate further extension. Multi-edge type density evolution-aided extrinsic information transfer chart is employed to predict the asymptotic performance during the base matrix extension and optimization. As an example, a rate-compatible RL-QC-LDPC code family with fine code-rate granularity is constructed via the proposed ECE. Compared with 5G-NR LDPC coded IDMA, the outage performance of enhanced IDMA with the new code family can be significantly improved at high user load and system throughput for NOMA-based random access.

INDEX TERMS 5G new radio access technology, interleave division multiple access (IDMA), non-orthogonal multiple access (NOMA), random access, raptor-like quasi-cyclic low-density parity-check (LDPC) code, rate-compatible.

I. INTRODUCTION

With the emergence of various Internet-of-Things (IoT) applications, including massive machine-type communications (mMTC) and ultra-reliable low latency communications (URLLC), 5G networks and beyond are expected to not only support significantly increased data traffic but also satisfy the requirements of massive connectivity, low latency, high reliability and/or diverse quality of service (QoS) [1], [2]. Random access has become an essential component in 5G due to its low latency and low scheduling overhead. From the viewpoint of network information theory [3], non-orthogonal multiple access (NOMA) is an elegant collision resolution scheme for random access. With joint decoding employed at the receiver, NOMA based random access is promising to provide higher reliability with low latency for URLLC applications compared with conventional random access methods. Besides, NOMA based random access can also support the

The associate editor coordinating the review of this manuscript and approving it for publication was Xueqin Jiang.

significantly increased user load by allowing the limited radio resources to be shared simultaneously by multiple users [4].

In order to approach the theoretical limit predicted by network information theory, well-designed channel codes are essential for practical NOMA schemes in scheduled access. For example, conventional interleave-division multiple-access (IDMA) with turbo-Hadamard codes, which is a capacity-approaching NOMA scheme with turbo joint decoding at the receiver, can achieve a gap of 1.4 dB to Shannon limit at the sum spectral efficiency of 1 bit/chip with 16 users [5]. Note that the channel resources are assumed to consist of orthogonal time-frequency resource elements, which are referred to as *chips* in this paper and most other related papers. With optimized repetition-aided irregular repeat-accumulate codes, IDMA can achieve a gap of 1.61 dB to Shannon limit supporting sum spectral efficiency of 2 bits/chip with 10 users [6]. To achieve good performance in random access, NOMA based random access schemes with practical channel codes also deserve investigation, and the robustness against the variations of user number should be taken into consideration.

Recently, rate-compatible raptor-like quasi-cyclic low-density parity-check (RL-QC-LDPC) codes have been recommended as the coding scheme of data channel for enhanced mobile broadband (eMBB) applications in 5G new radio (5G-NR) technical specification [7], [8]. Several novel structural features are incorporated into LDPC code design to fulfill the high-throughput and high-flexibility requirements of 5G-NR. The quasi-cyclic structure is particularly suitable for high-throughput applications and can also support scalable code block lengths [9]. In fact, QC-LDPC codes have also been adopted in several existing wireless standards, such as IEEE 802.16e [10], DVB-S2/T2/NGH [11]–[13] and DTMB [14]. The raptor-like structure is beneficial for providing rate compatibility and achieving capacity-approaching performance, especially at low code rates [15]. To further improve the threshold performance at high code rates, variable-node puncturing [16], [17] is employed, and the coded bits associated with the punctured variable nodes will not be transmitted. Owing to the rate compatibility, unprecedented granularity of code rates, code block lengths and information bit lengths has been achieved by 5G-NR LDPC codes, with only one or two code families defined by compact base matrices. Thus, the description and encoding/decoding implementation can be significantly simplified, and hybrid automatic repeat request (HARQ) can also be supported with the inherent incremental redundancy. Beside the industrial progress, there are also many works on construction of rate-compatible LDPC codes for point-to-point transmission in the literature, including rate-compatible protograph LDPC codes [18]–[21], LDPC convolutional codes [22]–[24], and spatially coupled LDPC codes [25], [26].

By incorporating rate-compatible RL-QC-LDPC codes into IDMA systems, enhanced IDMA has been recently developed as a highly flexible and capacity-approaching NOMA scheme in our preliminary works [27], [28]. The base matrices of RL-QC-LDPC code families were extended block by block for two or three compatible code rates in [27] and [28], and the corresponding degree distributions were optimized via differential evolution. This paper takes into consideration the novel structural features of the 5G-NR LDPC codes, and is focused on the construction of rate-compatible RL-QC-LDPC codes for enhanced IDMA based random access to flexibly support various spectral efficiencies with the robustness against the user-number variations. Instead of block-by-block extension with degree distribution optimization in [27] and [28], where the granularity of code rate/length is limited and the performance trade-off among different code rates is difficult, row-by-row extension method is adopted in this paper to construct a set of nested base matrices supporting a wide range of parity block lengths and code rates.

The idea of row-by-row extension has already been applied for rate-compatible RL-QC-LDPC code construction in point-to-point transmission system [18]–[21], and the base matrix optimization is primarily based on the asymptotic decoding threshold predicted by multi-edge type density evolution (DE) [15], [21], or the simplified versions, such as DE with reciprocal channel approximation (RCA) [20] and protograph-based extrinsic information transfer (EXIT) analysis [18], [19]. To obtain the decoding threshold of the code ensemble sharing the same base matrix, multi-edge type DE or RCA traces the iterative decoding procedure of the LDPC decoder according to the base matrix, and calculates the output reliability for underlying channel with the input signal-to-noise ratio (SNR).

However, since the iterations between multi-user detection (MUD) and LDPC decoding, i.e., the outer iterations, are essential for eliminating multi-user interference in enhanced IDMA, both the outer iterations and the iterations within the LDPC decoder, i.e., the inner iterations should be analyzed to obtain the asymptotic decoding threshold. For a given SNR, multiple output reliabilities of the LDPC decoder, corresponding to multiple input reliabilities from MUD in different outer iterations, need to be calculated to obtain the final output reliability of the turbo joint-decoding receiver. This leads to a significant increase in the complexity of calculating the decoding threshold for enhanced IDMA, compared with that for point-to-point transmission system. Therefore, it is hard to calculate the decoding thresholds for all candidate base matrices in the extension of each row. Meanwhile, there exists another tough issue for such a greedy extension algorithm, which is how to ensure good performance for different code rates in multiple extension rounds. Keeping more than one seed base matrix in each extension round could facilitate further extension, but the number of seed base matrices should also be limited to control the computational cost. To the best of our knowledge, it has not been disclosed how to efficiently select multiple effective seed base matrices, where enough diversity can be maintained for further base matrix extension.

In this paper, edge-classification based extension (ECE) algorithm is proposed to construct rate-compatible RL-QC-LDPC codes with fine code-rate granularity and moderate design complexity. ECE can address the issues of code construction for enhanced IDMA with the aid of two proposed edge-classification methods. The candidate base matrices are classified according to their edge-type spectra defined based on the edge-classification methods, which can efficiently reduce the total number of candidates and lower the computational complexity for each extension round. Then, owing to the reduced number of candidates, ECE employs beam search and keeps several representative candidates as seeds for next row extension, instead of only one seed [20]. Note that these seeds are selected based on not only the threshold performance, but also their edge-type spectra, which can maintain enough diversity in the group of the selected seeds and facilitate the search for good candidates in further extension rounds. The contributions of this paper can be summarized as follows.

Firstly, enhanced IDMA is developed as a NOMA based random access scheme in this paper, which can naturally support various single-user spectral efficiencies with the aid of rate-compatible RL-QC-LDPC codes. Enhanced IDMA can directly employ 5G-NR LDPC codes, called 5G-NR LDPC coded IDMA, and the performance is analyzed for random access as the baseline for the code construction. Besides, the combination of 5G-NR LDPC codes and NOMA based random access scheme could provide the compatibility for random access with other potential applications.

Secondly, to further improve the system throughput and user load in random access, ECE algorithm is proposed to construct rate-compatible RL-QC-LDPC codes towards enhanced IDMA. With the aid of two edge-classification methods, the extension and optimization of base matrices can be efficiently and effectively accelerated in ECE.

Thirdly, a new code family is constructed along with bit-repetition code via the proposed ECE algorithm for enhanced IDMA. Asymptotic analysis shows that enhanced IDMA with the constructed code family can support higher spectral efficiency compared with 5G-NR LDPC coded IDMA, while the rate compatibility is well maintained. The computational complexity of ECE algorithm is also analyzed during the construction process.

Finally, the block error rate (BLER) simulations are carried out to validate the individual outage performance of enhanced IDMA with the new code family in random access. The effect of bit-repetition code is also investigated.

II. SYSTEM MODEL AND CODE STRUCTURE

A. ENHANCED IDMA

Consider an uplink NOMA system, where multiple users transmit signals block-by-block to a single receiver. For random access, the number of arrivals at the receiver within a block is a random variable and can be modeled as a Poisson process. The probability of $J = J_0$ active users over a block

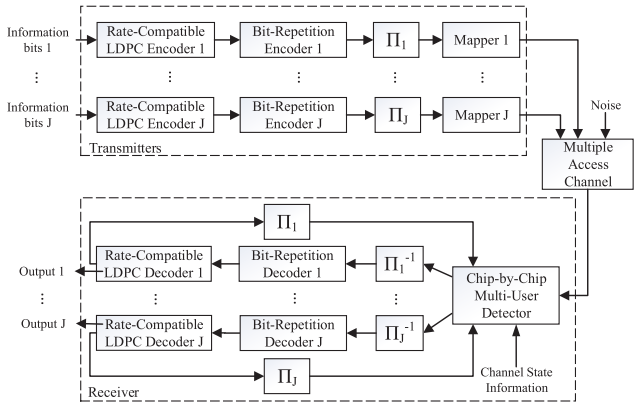

FIGURE 1. System model of enhanced IDMA.

can be expressed as

$$P_\lambda\left(J = J_0\right) = \frac{(\lambda)^{J_0}}{J_0!}e^{-\lambda}, \tag{1}$$

where $J_0 \geq 0$ and λ is the mean arrival rate per block, which is also called user load in the following.

The system model of enhanced IDMA for a given block with J active users is shown in Fig. 1, where J varies among different blocks in random access. Rate-compatible RL-QC-LDPC codes are employed to provide various code rates R_{L} for enhanced IDMA. The bit-repetition code with the code rate R_{rep} is optional for the cases requiring relatively low code rates, otherwise R_{rep} can be set to 1. With bit-interleaving, the concatenation of LDPC code and bit-repetition code can be regarded as a low-rate channel code, while the complexity of both code design and encoding/decoding can be significantly reduced compared with that of a low-rate LDPC code.

At the transmitters, the information bits of each user are independently encoded by the LDPC/bit-repetition encoder, bit-interleaved and mapped to constellation symbols. Then the constellation symbols of users are transmitted simultaneously over the chips, and the discrete-time memoryless equivalent baseband model for a block with J active users is given as

$$y = \sum_{j=1}^{J} h_j x_j + z, \tag{2}$$

where x_j and y are the transmitted symbol of user j and the received symbol, respectively, h_j is the normalized channel gain of user j with random phase rotation, and z is the zero-mean complex Gaussian noise. Gaussian multiple access channel with equal transmission power and equal spectral efficiency for each user is considered in this paper. This corresponds to one of the most challenging scenarios of multiple access, where there exists equally strong multi-user interference for each user. Binary phase shift keying (BPSK) is assumed for all users for simplicity.

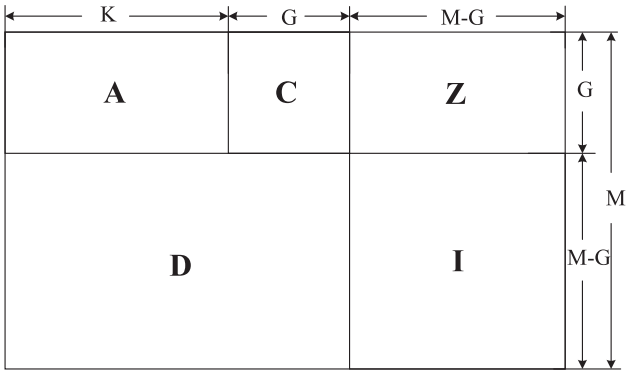

FIGURE 2. The structure of base matrix B for RL-QC-LDPC codes.

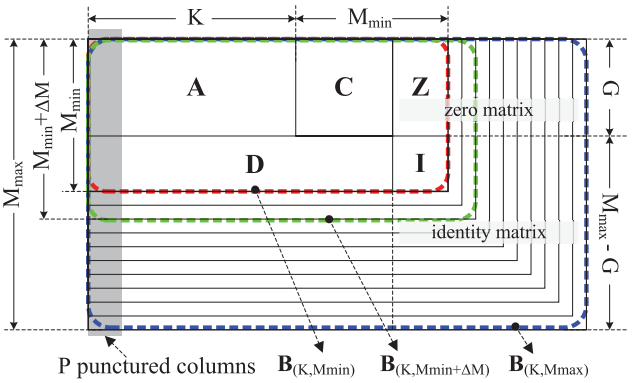

FIGURE 3. The nested base matrices of a rate-compatible RL-QC-LDPC code family supporting $M_{min} \le M \le M_{max}$.

At the receiver, the chip-by-chip multi-user detection (MUD) and channel decoding, including the LDPC and bit-repetition decoding, are performed iteratively. Elementary signal estimator (ESE) [5] is an efficient chip-by-chip multi-user detector to support a large number of users with low complexity. Specially, for the cases with a small number of users transmitting at relatively high spectral efficiency, symbol-by-symbol or, equivalently, chip-by-chip MAP multi-user detector can be adopted in enhanced IDMA instead of ESE for better performance [27].

B. RATE-COMPATIBLE RL-QC-LDPC CODE

A conventional LDPC code can be defined by its parity check matrix of size $m \times (k+m)$, where k and m are the information and parity bit lengths, respectively. Accordingly, the code block length is $k + m$ and the code rate is $k/(k + m)$. For a QC-LDPC code, the parity check matrix can be constructed by lifting the $M \times (K + M)$ base matrix, which is also called protograph [17], [29]. In lifting process, the zeros and ones of the base matrix are replaced by zero matrices and circulant permutation matrices of size $L \times L$. With one or multiple sets of lifting factors L, scalable information bit lengths $k = KL$, parity bit lengths $m = ML$ and code block lengths $(K + M)L$ can be supported [9], [30].

For RL-QC-LDPC codes, more structural features are incorporated into the base matrix **B**, as shown in Fig. 2, which can be regarded as the concatenation of the base matrices of a precode [**A C**] and a Luby Transform code [**D I**]. The submatrices **Z** and **I** are zero matrix and identity matrix, respectively. The size of [**A C**] is $G \times (K + G)$, where G is usually assumed to be small to provide relatively high code rate for the precode. By allowing multiple degree-one columns added in the base matrix **B**, the rate compatibility can be supported, and the performance of RL-QC-LDPC codes can be improved, especially at low code rates. Owing to the raptor-like structure, only the entries in submatrices [**A C**] and **D** need to be designed. RL-QC-LDPC codes have been employed in the latest broadcasting standard ATSC 3.0 [31]. Although the parity check matrices in ATSC 3.0 are independently designed for different code rates and code block lengths, RL-QC-LDPC codes are inherently suitable for rate compatibility due to degree-one parity variable nodes associated with submatrix **I**.

Recently, instead of the turbo codes in 3G and 4G, LDPC codes have been adopted for the data channel of eMBB applications in 5G-NR [7], [8]. The 5G-NR LDPC codes incorporate not only the RL-QC structure but also the feature of rate compatibility. Owing to the incremental redundancy, 5G-NR LDPC codes are capable of providing a wide range of code rates and code block lengths and facilitating HARQ. To improve the threshold performance, variable-node puncturing [16], [17] is also employed for 5G-NR LDPC codes. More specifically, if P columns of the base matrices are assumed to be punctured, the coded bits associated with the P punctured columns will not be transmitted. Accordingly, the code block length is changed to $(K + M - P)L$, and the code rate is changed to $K/(K + M - P)$.

To construct rate-compatible RL-QC-LDPC codes for point-to-point transmission, there are mainly two approaches, puncture [32], [33] and extension [20], [28]. In [32] and [33], the lowest-rate code was designed first and punctured to obtain other codes with higher rates. In [20], given a fixed information block length K for the base matrices, the smallest base matrix of the highest-rate code was designed first, and extended row by row to construct larger base matrices with consecutive parity block lengths M for lower code rates. Furthermore, a two-dimensional extension method called progressive matrix growth (PMG) was proposed in [28] to construct rate-compatible base matrices providing the scalability of both information and parity block lengths.

Since the row-by-row extension method is employed for code construction in this paper, the structure of the nested base matrices for such a rate-compatible RL-QC-LDPC code family is given in Fig. 3, where $\mathbf{B}_{(K,M)}$ denotes the base matrix of size $M \times (K + M)$. Specifically, the information block length is K, and consecutive parity block lengths M, from $M_{\min}$ to $M_{\max}$, can be supported with the nested base matrices. Note that the minimum parity check length $M_{\min}$ is required to be larger than or equal to G. Based on the

smallest $\mathbf{B}_{(K,M_{\min})}$, larger base matrix $\mathbf{B}_{(K,M_{\min}+\Delta M)}$ can be obtained by extending ΔM rows and maintaining the raptor-like structure. With the P columns of the base matrices assumed to be punctured, code rates from $K/(K+M_{\max}-P)$ to $K/(K+M_{\min}-P)$ can be provided with the code family in Fig. 3.

III. EDGE-CLASSIFICATION BASED EXTENSION ALGORITHM

In this section, two edge-classification methods, called *EC-I* and *EC-II*, are first proposed, and the corresponding edge-type spectra for base matrices can be calculated. Then the ECE algorithm is developed with the aid of these two edge-classification methods. ECE can efficiently and effectively accelerate the greedy row extension and base matrix optimization process for rate-compatible RL-QC-LDPC code families, while maintaining enough diversity in the seed base matrices for further row extension.

A. TWO EDGE-CLASSIFICATION METHODS

For an RL-QC-LDPC code ensemble, the base matrix represents a bipartite graph called base graph. The columns, rows and non-zero entries of the base matrix correspond to the variable nodes, check nodes and edges in the base graph, respectively. As shown in Fig. 3, extending each row of $\mathbf{B}_{(K,M)}$ is equivalent to adding a check node and a degree-one parity variable node into the corresponding base graph. And the connections between the added check node and the variable nodes, associated to the precode [**A C**], need to be designed.

For each edge in the base graph represented by $\mathbf{B}_{(K,M)}$, the degrees of the connected variable node and check node are denoted by v and c, respectively. Since variable-node puncturing is employed in this paper, the channel type p of each edge is determined by the connected variable node. Specifically, if the connected variable node is punctured, $p=1$, otherwise, $p=0$. By jointly considering these three characteristics of the edges, the edge type for the first edge-classification method EC-I is defined by the 3-tuple (p, v, c), which means the edges with the same channel type p and degrees of the connected variable node v and check node c are classified into the same type (p, v, c). Based on the definition of EC-I edge type, the EC-I edge-type spectrum for $\mathbf{B}_{(K,M)}$ is defined as

$$E_{\mathrm{I}}(\alpha,\beta,\gamma)=\sum_{p,v,c}\rho_{p,v,c}\alpha^{p}\beta^{v}\gamma^{c}, \tag{3}$$

where $\rho_{p,v,c}$ represents the ratio of type-(p, v, c) edges to all the edges of $\mathbf{B}_{(K,M)}$, and α, β and γ are three dummy variables.

In edge-classification method EC-II, the edge type is defined by the tuple (p, v), which only considers the channel type and the degree of the connected variable node. Similarly, the EC-II edge-type spectrum for $\mathbf{B}_{(K,M)}$ is defined as

$$E_{\mathrm{II}}(\alpha,\beta)=\sum_{p,v}\rho_{p,v}\alpha^{p}\beta^{v}, \tag{4}$$

where $\rho_{p,v}$ represents the ratio of type-(p, v) edges to all the edges of $\mathbf{B}_{(K,M)}$, and α and β are dummy variables. Since $\rho_{p,v}=\sum_{c}\rho_{p,v,c}$, EC-I can be regarded as EC-II with further classification based on the degree of connected check node.

B. THE PROPOSED ECE ALGORITHM

For the base matrix optimization during the greedy row-by-row extension, the gap of asymptotic decoding threshold $\mathrm{SNR}_{\text{DE-EXIT}}$ to corresponding Shannon limit $\mathrm{SNR}_{\mathrm{Shan}}$ is considered as an important metric in ECE. To calculate asymptotic decoding threshold $\mathrm{SNR}_{\text{DE-EXIT}}$ of a specific base matrix for enhanced IDMA, multi-edge type DE aided EXIT (DE-EXIT) chart [28] is adopted. Unlike conventional multi-edge type DE or its simplified versions, which usually focus on calculating the output reliability of the LDPC decoder for a given input reliability or SNR from the underlying channel, DE-EXIT analysis considers both the inner iterations within the LDPC decoder and the outer iterations between the LDPC decoder and MUD. DE-EXIT chart consists of the EXIT curve of MUD and the inverted EXIT curve of channel decoding, which can be obtained by calculating the output reliabilities for multiple input reliabilities via multi-edge type DE. Since an EXIT curve can establish the relationship between the input a priori information and the output extrinsic information of a module, the iterative procedure between MUD and channel decoding can be visualized through the trajectory between the corresponding two EXIT curves. And the first intersection of these two EXIT curves represents the final output reliability of the turbo joint-decoding receiver for enhanced IDMA. With Gaussian approximation assumed, the final output bit error rate can be further obtained.

As a result, the complexity of calculating the asymptotic decoding threshold of enhanced IDMA increases significantly compared with that for point-to-point transmission system. To construct the nested base matrices in Fig. 3 via row-by-row extension, $K+G$ entries need to be designed for each extension round. Firstly, the maximum and minimum degrees of each extended row are pre-determined in ECE to reduce the number of candidate base matrices. Then ECE classifies the candidate base matrices with the aid of EC-I to avoid calculating decoding thresholds for all of them. Specifically, given a set of candidate base matrices $\{\mathbf{B}_{(K,M)}\}$ of the same size $M\times(K+M)$, the corresponding EC-I edge-type spectra can be calculated by (3). Since the threshold performance of the base matrices with the same EC-I edge-type spectrum is very close, only one of them is selected as the representative candidate base matrix, and analyzed for the corresponding EC-I edge-type spectrum in ECE.

Since the nested base matrices are progressively constructed with a greedy extension algorithm, it is challenging how to ensure good performance for different code rates in multiple extension rounds. In [20], several constraints on edge connection were imposed to facilitate effective extension of the base matrices, and one candidate with the smallest threshold gap under these constraints was kept in each row extension. Unlike the algorithm in [20], ECE employs

beam search and selects multiple seed base matrices in each extension round. However, if the diversity in the selected seeds is not enough, the row-by-row extension with these ineffective seeds may still fail to achieve the performance trade-off in multiple extension rounds. In this paper, the seeds are selected jointly based on their EC-I and EC-II edge-type spectra and decoding thresholds, which can provide enough diversity for further row extension. In other words, ECE intends to select the candidate base matrices with not only small decoding threshold gaps $\mathrm{SNR}_{\text{DE-EXIT}} - \mathrm{SNR}_{\text{Shan}}$, but also distinct EC-I and EC-II edge-type spectra.

The basic procedures of ECE are summarized in the following. Firstly, the precode of size $G\times(K+G)$ is designed via conventional methods, and one or more candidate precodes are selected as seed base matrices for the following row-by-row extension. Secondly, perform the row-by-row extension as shown in Algorithm 1 to progressively extend the seed base matrices to each $M = G+1, G+2, \ldots, M_{\max}$. The output n_{seed} base matrices of Algorithm 1 for extending the base matrices to $M-1$ are used as the input seeds of Algorithm 1 for extending the base matrices to M. Note that the target number of users J_{target} for Algorithm 1 can be varying for different target parity block length M. Finally, from all the output base matrices of the extension round to $M_{\max}$, the base matrix with the smallest threshold gap is selected as the final result.

To illustrate the row-by-row extension in Algorithm 1 more clearly, an example of extending the base matrices from $M-1$ to M is given in the following. Assume that the set of n_{seed} seed base matrices obtained from the last extension round is denoted by $\{\mathbf{B}^{\text{seed}}_{(K,M-1)}\}$. Firstly, the set of candidate base matrices $\{\mathbf{B}_{(K,M)}\}$ can be generated by extending a row for all seeds in $\{\mathbf{B}^{\text{seed}}_{(K,M-1)}\}$, with the constraints of maximum and minimum degrees of the extended row, i.e., $c_{\max}$ and $c_{\min}$, respectively. Secondly, the EC-II edge-type spectra of all candidates in $\{\mathbf{B}_{(K,M)}\}$ are calculated, and $\{\mathbf{B}_{(K,M)}\}$ is divided into n_{II} subsets $\{\mathbf{B}_{(K,M)}\}^i_{\text{II}}$, $i = 1, 2, \ldots, n_{\text{II}}$, which correspond to the n_{II} unique EC-II edge-type spectra. Thirdly, for the candidates in each subset $\{\mathbf{B}_{(K,M)}\}^i_{\text{II}}$ with the same EC-II edge-type spectrum, the EC-I edge-type spectra are calculated, and only one base matrix is selected as the representative candidate for each different EC-I edge-type spectrum. For the representative candidates in each subset $\{\mathbf{B}_{(K,M)}\}^i_{\text{II}}$ with the same EC-II edge-type spectrum, the corresponding decoding threshold gaps are calculated, and the one with the smallest threshold gap is selected and added into the list $\mathcal{L}_{\text{matirx}}$. Finally, the n_{seed} base matrices with the smallest threshold gaps are selected as the seed base matrices for next extension round, and added into $\{\mathbf{B}^{\text{seed}}_{(K,M)}\}$.

In general, edge-classification method EC-I is utilized to reduce the number of candidates to be analyzed, and hence improves the computational efficiency of each row extension; edge-classification method EC-II is utilized to ensure the diversity in the selected seeds for further extension rounds, and hence improves the effectiveness of performance trade-off in the successive extension procedure.

Algorithm 1 Edge-Classification Based Extension

Inputs: The set of n_{seed} seed base matrices $\{\mathbf{B}^{\text{seed}}_{(K,M-1)}\}$; The target parity block length M; The maximum and minimum degrees, $c_{\max}$ and $c_{\min}$, of the row to be extended; The target number of users J_{target}.

Output: The output set of n_{seed} base matrices $\{\mathbf{B}^{\text{seed}}_{(K,M)}\}$.

1: Initialize two empty lists $\mathcal{L}_{\text{gap}}$ and $\mathcal{L}_{\text{matirx}}$, and an empty set $\{\mathbf{B}^{\text{seed}}_{(K,M)}\}$.
2: Extend all seeds in $\{\mathbf{B}^{\text{seed}}_{(K,M-1)}\}$ from $M-1$ to M with constraints of $c_{\max}$ and $c_{\min}$, and generate the set $\{\mathbf{B}_{(K,M)}\}$ of all candidate base matrices.
3: Calculate EC-II edge-type spectra for all candidates in $\{\mathbf{B}_{(K,M)}\}$.
4: According to the EC-II edge-type spectra, classify the candidates in $\{\mathbf{B}_{(K,M)}\}$ into n_{II} subsets $\{\mathbf{B}_{(K,M)}\}^i_{\text{II}}$, $i = 1, 2, \ldots, n_{\text{II}}$.
5: **for** $i = 1;\ i \le n_{\text{II}};\ i++$ **do**
6: Calculate EC-I edge-type spectra for all candidates in $\{\mathbf{B}_{(K,M)}\}^i_{\text{II}}$.
7: According to the EC-I edge-type spectra, classify the candidates in $\{\mathbf{B}_{(K,M)}\}^i_{\text{II}}$.
8: Choose one representative candidate for each different EC-I edge-type spectrum.
9: Calculate the decoding threshold gaps of all representative candidates for the target number of users J_{target}.
10: Select the smallest threshold gap, and add the threshold gap and the corresponding base matrix into $\mathcal{L}_{\text{gap}}$ and $\mathcal{L}_{\text{matirx}}$, respectively.
11: **end for**
12: Select the n_{seed} minimum threshold gaps from $\mathcal{L}_{\text{gap}}$ and the corresponding base matrices from $\mathcal{L}_{\text{matirx}}$.
13: Add these n_{seed} base matrices into $\{\mathbf{B}^{\text{seed}}_{(K,M)}\}$.

The n_{seed} seeds in $\{\mathbf{B}^{\text{seed}}_{(K,M)}\}$ are the representative candidates of their EC-I edge-type spectra, and meanwhile, each one of them also represents a different EC-II edge-type spectrum. Instead of choosing the n_{seed} candidates with the smallest threshold gaps from $\{\mathbf{B}_{(K,M)}\}$, ECE selects one candidate with the smallest threshold gap from the subset $\{\mathbf{B}_{(K,M)}\}^i_{\text{II}}$ for each EC-II edge-type spectrum, and then determines the final output n_{seed} base matrices among these effective candidates to achieve the performance tradeoff in multiple extension rounds. In this way, ECE is developed as an efficient and effective row-by-row extension algorithm for finding good rate-compatible RL-QC-LDPC code families towards enhanced IDMA, as demonstrated by the following example of code construction in Section IV.

IV. PERFORMANCE ANALYSIS AND CODE CONSTRUCTION

In this section, firstly, the theoretical and practical individual outage performance of 5G-NR LDPC coded IDMA in random access is analyzed, which can provide insights on

code construction and optimization towards enhanced IDMA based random access. Secondly, based on the individual outage analysis, a new rate-compatible RL-QC-LDPC code family (*new code family* for short) is constructed via the proposed ECE algorithm to improve the supported system throughput and user load for 5G-NR LDPC coded IDMA, while maintaining the fine code-rate granularity. During the construction process, the computational complexity of ECE is also discussed. Thirdly, with the aid of DE-EXIT chart, the asymptotic performance and robustness against the variations of user number are carefully analyzed for enhanced IDMA with the new code family as well as 5G-NR LDPC codes. Finally, BLER simulations are carried out to validate the performance of enhanced IDMA with the new code family in random access, which is also compared with that of 5G-NR LDPC coded IDMA.

A. THEORETICAL OUTAGE ANALYSIS AND 5G-NR LDPC CODED IDMA

In enhanced IDMA with BPSK employed, the single-user spectral efficiency can be represented by $\eta_{\mathrm{u}} = R_{\mathrm{L}} R_{\mathrm{rep}}$. As described in (1), the number of active users J over a block is modeled as a Poisson process for random access. Then the average sum spectral efficiency of enhanced IDMA in random access can be defined as $\eta_{\mathrm{s}}^{\mathrm{avg}} = \lambda \eta_{\mathrm{u}}$. Given the user load λ and the target single-user spectral efficiency η_{u}, the theoretical individual outage probability of enhanced IDMA can be calculated by analyzing the individual outage behavior of such a turbo joint-decoding receiver with ideal coded modulation for different E_{b}/N_0 [34], [35]. Since this paper is focused on mMTC scenario, the thresholds are mainly obtained at individual outage probability of $p_{\mathrm{out}} = 0.1$, as recommended for link level simulation of mMTC in [36]–[38].

Firstly, the average sum spectral efficiency of $\eta_{\mathrm{s}}^{\mathrm{avg}} = 0.3$ bits/chip is considered, and the theoretical individual outage probability curves with Gaussian inputs for different single-user spectral efficiencies of $\eta_{\mathrm{u}} = \{1/4, 1/8, 1/16\}$ bits/chip are obtained and given in Fig. 4, where the user loads are $\lambda = \{1.2, 2.4, 4.8\}$, respectively. For the given E_{b}/N_0 and $\eta_{\mathrm{s}}^{\mathrm{avg}}$, the individual outage probability becomes lower as single-user spectral efficiency decreases, or equivalently, as user load increases. To achieve the target $\eta_{\mathrm{s}}^{\mathrm{avg}} = 0.3$ bits/chip, the required E_{b}/N_0 are -0.74, -0.57 and -0.06 dB at $p_{\mathrm{out}} = 0.1$ for $\eta_{\mathrm{u}} = \{1/4, 1/8, 1/16\}$ bits/chip, respectively.

The practical individual outage performance of 5G-NR LDPC coded IDMA is also analyzed, which can be regarded as the baseline for the following code construction. The 5G-NR LDPC codes utilized in this paper are from base graph 2 [7], and the corresponding nested base matrices are given in Fig. 5, where the squares and crosses denote ones and zeros, respectively. The code family with $K = 10$ and $M = \{17, 18, \ldots, 42\}$ is mainly considered, and the first $P = 2$ columns are punctured to improve the threshold performance. Accordingly, the supported LDPC code rates $R_{\mathrm{L}} = K/(K + M - P)$ are from 2/5 down to 1/5.

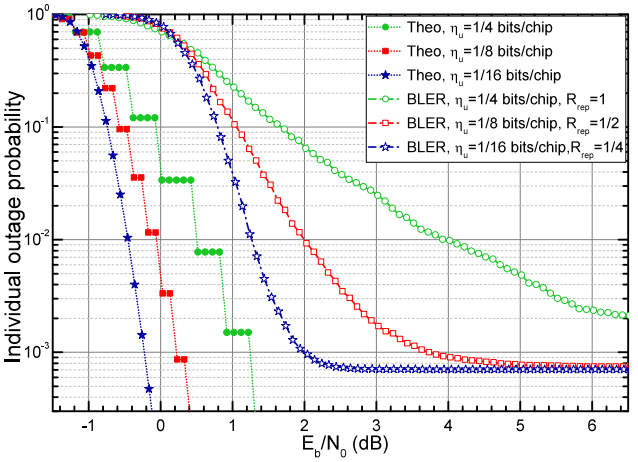

FIGURE 4. Individual outage probability for average sum spectral efficiency of $\eta_{\mathrm{s}}^{\mathrm{avg}} = 0.3$ bits/chip with different single-user spectral efficiencies η_{u}, from theoretical outage analysis and BLER simulations for 5G-NR LDPC coded IDMA with $R_{\mathrm{L}} = 1/4$ and $R_{\mathrm{rep}} = \{1, 1/2, 1/4\}$.

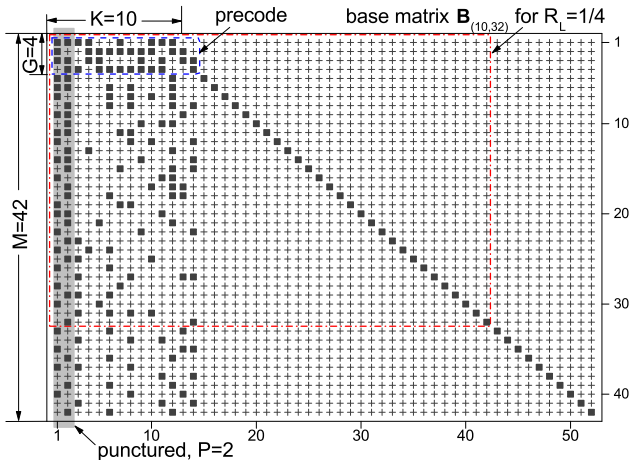

FIGURE 5. The nested base matrices of 5G-NR LDPC code family.

To compare with the theoretical outage analysis for $\eta_{\mathrm{s}} = 0.3$ bits/chip, the 5G-NR LDPC code of $R_{\mathrm{L}} = 1/4$ is combined with bit-repetition codes of $R_{\mathrm{rep}} = \{1, 1/2, 1/4\}$ to provide single-user spectral efficiencies of $\eta_{\mathrm{u}} = \{1/4, 1/8, 1/16\}$ bits/chip. The practical individual outage probability of 5G-NR LDPC coded IDMA in random access can be obtained by calculating the weighted BLER with respect to the Poisson distributed arrivals. In BLER simulations, the number of outer iterations between MUD and channel decoding is set as 15. In each outer iteration, channel decoding performs 1 bit-repetition decoding and 6 inner iterations within the LDPC decoder, and then transfers extrinsic information to MUD [39]. The lifting factor is set as $L = 32$, and thus the information bit length is as short as $k = 320$ bits for each code rate. Note that, with the short information bit length, the discussions in this paper could provide insights for practical applications, like small-packet transmission in mMTC.

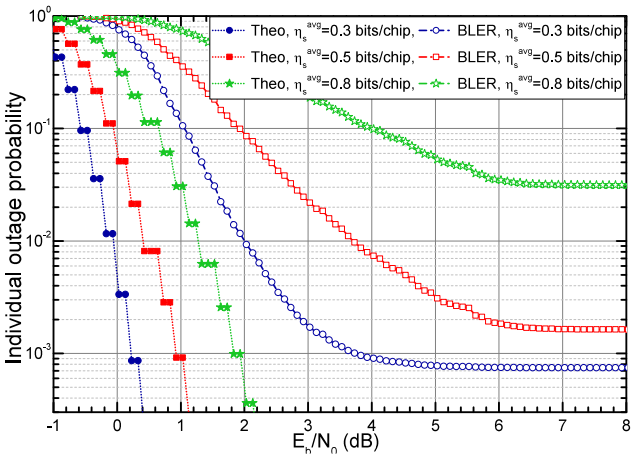

FIGURE 6. Individual outage probability for different average sum spectral efficiencies η_s^{avg} with single-user spectral efficiency of $\eta_u = 1/8$ bits/chip, from theoretical outage analysis and BLER simulations for 5G-NR LDPC coded IDMA with $R_L = 1/4$ and $R_{rep} = 1/2$.

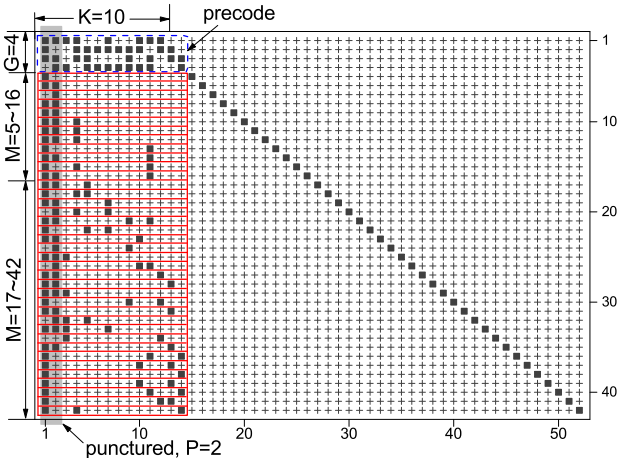

FIGURE 7. The nested base matrices of the constructed rate-compatible RL-QC-LDPC code family.

With $\lambda = \{1.2, 2.4, 4.8\}$, the individual outage probability curves of 5G-NR LDPC coded IDMA for $\eta_u = \{1/4, 1/8, 1/16\}$ bits/chip are also shown in Fig. 4. The BLER simulation results of 5G-NR LDPC coded IDMA are in accordance with the theoretical analysis. Given $\eta_s^{avg} = 0.3$ bits/chip, the E_b/N_0 threshold at $p_{out} = 0.1$ is 1.65 dB for $\eta_u = 1/4$ bits/chip, and decreases to 1.03 and then 0.80 dB for $\eta_u = 1/8$ and $1/16$ bits/chip, respectively. The theoretical analysis and BLER simulation results both indicate that the individual outage performance can be improved with lower single-user spectral efficiency for a given average sum spectral efficiency. The simple explanation is that, as the user load increases, the user variation will be decreased according to the central limit theorem, and the outage performance will be improved accordingly.

Secondly, the theoretical and practical individual outage performance is analyzed for different average sum spectral efficiencies. Take 5G-NR LDPC coded IDMA with $R_L = 1/4$ and $R_{rep} = 1/2$ as an example. The user loads are $\lambda = \{2.4, 4, 6.4\}$ for $\eta_s^{avg} = \{0.3, 0.5, 0.8\}$ bits/chip, respectively. The theoretical and practical individual outage probability curves for these three cases are shown in Fig. 6. At $p_{out} = 0.1$, the gap of E_b/N_0 threshold from BLER simulations to the E_b/N_0 threshold from theoretical analysis is only 1.60 dB for $\eta_s^{avg} = 0.3$ bits/chip. However, the gap increases to 2.06 dB for $\eta_s^{avg} = 0.5$ bits/chip, and 3.51 dB for $\eta_s^{avg} = 0.8$ bits/chip. As shown in Fig. 4, the gaps for $\eta_s^{avg} = 0.3$ bits/chip are also only 1.71 and 1.54 dB with $\eta_u = 1/4$ and $1/16$ bits/chip. This means that 5G-NR LDPC coded IDMA can support relatively low average sum spectral efficiency and user load with good performance in random access, but faces server performance degradation at high average sum spectral efficiency and user load. Moreover, at $p_{out} = 0.01$ in Fig. 4 and Fig. 6, the corresponding gaps become larger, or even cannot be obtained for some cases due to the floors on the curves. These floors could be caused by the short code length, incorporation of bit-repetition, or code construction method/criterion. Thus, for scenarios requiring much higher reliability, like URLLC, the channel codes need to be specially constructed towards much lower error floor.

B. CODE CONSTRUCTION WITH ECE ALGORITHM

According to the theoretical outage analysis in Section IV-A, it is beneficial to construct the rate-compatible RL-QC-LDPC code family along with bit-repetition code, which can provide relatively low code rate and improve individual outage performance at the given average sum spectral efficiency. With the aid of bit-repetition code, the nested base matrices of the RL-QC-LDPC code family can still be compact to reduce the description and implementation complexity. However, for a given average sum spectral efficiency, the user load increases as the single-user spectral efficiency decreases, which will lead to higher complexity at the receiver of enhanced IDMA. Therefore, the bit-repetition code of $R_{rep} = 1/2$ is incorporated into the code construction in this subsection.

The size of the newly constructed rate-compatible RL-QC-LDPC code family is set the same as that of the utilized 5G-NR LDPC code family, i.e., $K = 10$, $G = 4$, $P = 2$ and $M_{max} = 42$. The new code family is constructed via ECE algorithm, and the corresponding base matrices are shown in Fig. 7 to help illustrate the construction process more clearly. As described in Section III-B, the threshold gap $\mathrm{SNR}_{\text{DE-EXIT}} - \mathrm{SNR}_{\text{Shan}}$ is utilized as the performance metric in ECE algorithm. To obtain the asymptotic decoding threshold $\mathrm{SNR}_{\text{DE-EXIT}}$ via DE-EXIT analysis, the output bit error rate is required to be less than 10^{-3} in this paper. The Shannon limit $\mathrm{SNR}_{\text{Shan}}$ is the theoretical limit of Gaussian multiple access channel with Gaussian input, which can be calculated as $\mathrm{SNR}_{\text{Shan}} = 10\log_{10}(2^{\eta_s} - 1)$ (dB) for sum spectral efficiency of η_s.

For simplicity, the 4×14 precode of 5G-NR LDPC code family is directly adopted as the precode for the new code family. Then the 5G-NR LDPC precode are progressively

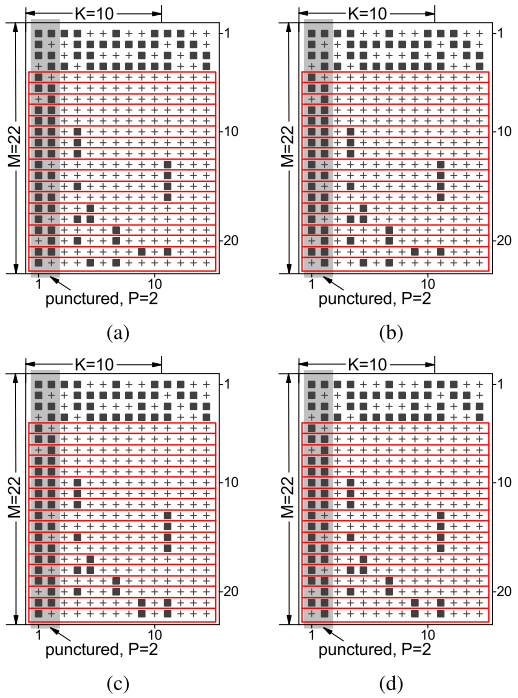

FIGURE 8. The $n_{seed} = 4$ selected seed base matrices for row extension to $M = 23$ in ECE. For simplicity, only the first 14 columns are shown.

extended for $M = 5$–42 row by row to construct the nested base matrices for the new code family. To improve the performance at high average sum spectral efficiency and user load, the target user number $J_{target} = 18$ is considered for the primary code rates of the new code family. However, DE-EXIT analysis shows that the smallest threshold gap of the original 5G-NR LDPC code for $M = 5$ and $R_{rep} = 1/2$ is obtained with $J = 2$ users, and the design freedom is limited for the extension of precode from $M = 4$ to $M = 5$. Therefore, it is difficult to directly construct the base matrix of the new code family towards $J_{target} = 18$ for $M = 5$, and $J_{target} = 6$ is selected instead. To ensure efficient base matrix extension while gradually increasing the target user number, $J_{target} = M + 1$ is adopted for each M from 5 to 16. Then the target user number of $J_{target} = 18$ can be applied for further extension to $M = 17, 18, \ldots, 42$, corresponding to the code rates within 1/5–2/5. Moreover, during the row-by-row extension, the maximum degree c_{max} of the row is set as 5 and 4 for $M = 5$–35 and $M = 36$–42, respectively, the minimum degree c_{min} of the row is set as 2, and $n_{seed} = 4$ seed base matrices are assumed to be kept for each extension round.

Based on the base matrix extension from $M = 22$ to $M = 23$, the computational complexity of ECE algorithm is briefly analyzed. Since calculating the decoding thresholds for different candidate base matrices in enhanced IDMA system requires most of the computing resources, we mainly focus on the reduction of candidate base matrices during the extension process. To extend the base matrix from $M = 22$ to $M = 23$, one row needs to be added to the $n_{seed} = 4$ seed base matrices of size 22×32, which are given in Fig. 8.

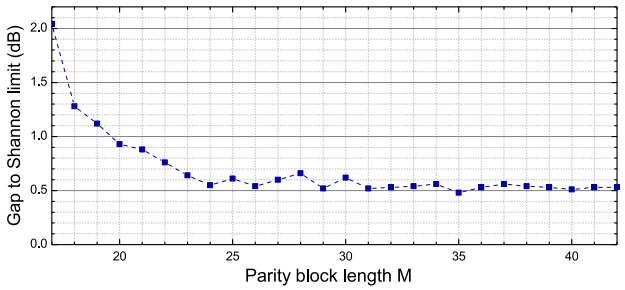

FIGURE 9. Gap of asymptotic threshold to Shannon limit vs. parity block length M, predicted by DE-EXIT analysis.

Constrained by the raptor-like structure, the entries in the 1st–14th columns of the 23rd row are required to be optimized. Firstly, without any constraints of the entries, there are totally $n_{seed} \times 2^{14} = 65536$ candidate base matrices. Secondly, with the constraints of $c_{max} = 5$ and $c_{min} = 2$, the number of ones in the 23rd row and 1st–14th columns can only be 4, 3, 2 or 1, and hence the number of candidate base matrices is reduced to 5880. Thirdly, by classifying the candidate base matrices according to their EC-I edge-type spectra, the number of candidate base matrices can be further reduced to 1457. As we can see, with the constraints on maximum and minimum degrees of the extended row and the edge-classification method EC-I, the number of candidate base matrices can be significantly reduced for ECE algorithm.

Moreover, among the 5880 candidate base matrices obtained with $c_{max} = 5$ and $c_{min} = 2$, there are only 586 different EC-II edge-type spectra. Without edge-classification methods EC-I and EC-II, the seed base matrices will be directly selected from the 5880 candidate base matrices, and could have the same EC-II edge-type spectrum, or even the same EC-I edge-type spectrum, which means limited diversity and may impair the effect of keeping multiple seeds in the extension procedure. Thus, ECE algorithm selects no more than one seed base matrix for each of the 586 EC-II edge-type spectra. In this way, the effectiveness of the selected seed base matrices can be ensured for the following extension from $M = 23$ to $M = 24, 25, \ldots, 42$.

C. ASYMPTOTIC ANALYSIS

Via DE-EXIT analysis, the asymptotic decoding thresholds for the primary code rates $R_L = K/(K + M - P)$, $M = 17$–42, of the new code family are obtained, with $R_{rep} = 1/2$ and the target user number $J_{target} = 18$. The gaps of the asymptotic decoding threshold to Shannon limit are depicted in Fig. 9. Using the same 5G-NR LDPC precode, the target user numbers for $M = 5$–17 in ECE are gradually increased from 6 to the final 18. For $M = 17$–22 with $J_{target} = 18$, the thresholds in Fig. 9 become closer to Shannon limit as M decreases thanks to the increasing design freedom, and for $M = 23$–42, the threshold gaps are less than 0.70 dB.

Then the asymptotic performance of enhanced IDMA with the new code family and 5G-NR LDPC code family is

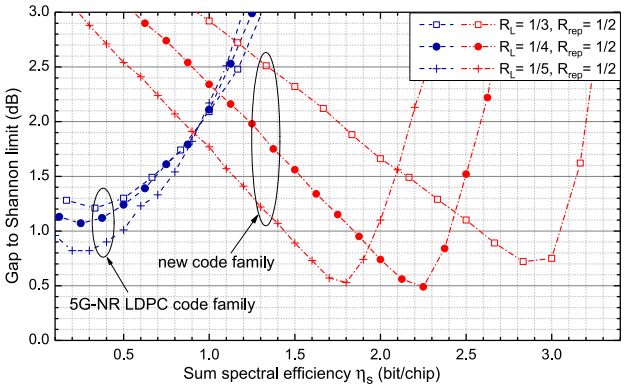

FIGURE 10. Gap of asymptotic threshold to Shannon limit vs. sum spectral efficiency η_S, predicted by DE-EXIT analysis.

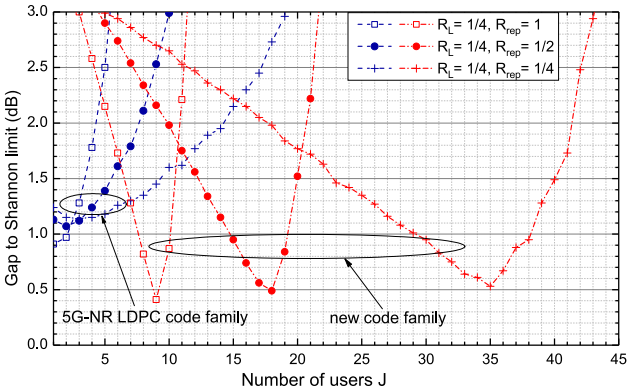

FIGURE 11. Gap of asymptotic threshold to Shannon limit vs. number of users J, predicted by DE-EXIT analysis.

compared for different sum spectral efficiencies. With bit-repetition code of $R_{\text{rep}} = 1/2$ employed, the LDPC codes of $R_{\text{L}} = \{1/3, 1/4, 1/5\}$ are analyzed as examples, corresponding to single-user spectral efficiencies of $\eta_{\text{u}} = 0.17$, 0.125 and 0.10 bits/chip. Different sum spectral efficiencies can be obtained with different numbers of users, and the corresponding threshold gaps are shown in Fig. 10.

For 5G-NR LDPC code family, the asymptotic decoding thresholds for all three LDPC code rates are relatively close to Shannon limit at sum spectral efficiency $\eta_{\text{s}} \leq 0.50$ bits/chip. However, the asymptotic performance of 5G-NR LDPC codes significantly degrades at $\eta_{\text{s}} > 0.50$ bits/chip, which is because the 5G-NR LDPC code family is mainly optimized for point-to-point transmission and the target sum spectral efficiency is relatively low for $R_{\text{L}} = \{1/3, 1/4, 1/5\}$.

For the three LDPC codes from the new code family, which are constructed with $J_{\text{target}} = 18$, the smallest threshold gaps of enhanced IDMA with the new code family are achieved at much higher sum spectral efficiencies. As a result, the asymptotic performance for the new code family is worse than that of the 5G-NR LDPC codes at relatively low sum spectral efficiency, but the maximum sum spectral efficiencies for $R_{\text{L}} = \{1/3, 1/4, 1/5\}$ are significantly improved with the new code family, given the maximum threshold gap of 2.00 dB. More specifically, the maximum sum spectral efficiencies are within 0.90 bits/chip for all three LDPC code rates from the 5G-NR LDPC code family. At the same time, the maximum sum spectral efficiency is 2.10 bits/chip for the new code family with $R_{\text{L}} = 1/5$, and can be further increased to 2.50 and 3.17 bits/chip for $R_{\text{L}} = 1/4$ and $1/3$, respectively.

Since the new code family is constructed for enhanced IDMA based random access, the robustness against the variations of user number should also be analyzed. Taking $R_{\text{L}} = 1/4$ as an example, the asymptotic threshold gaps of enhanced IDMA with the new code family and 5G-NR LDPC code family for different user numbers are given in Fig. 11, where different bit-repetition code rates are also considered. Without bit-repetition code, i.e., $R_{\text{rep}} = 1$, the range of supported user number is only 1–4 for 5G-NR LDPC code, given the maximum threshold gap of 2.00 dB. With $R_{\text{rep}} = 1/2$ and $1/4$, the ranges are extended to 1–7 and 1–14, respectively. Thus, 5G-NR LDPC coded IDMA can be robust against the variations of user number for relatively low user load with the aid of bit-repetition code. For enhanced IDMA with the new code family, the ranges of supported user number are 6–10, 10–20 and 18–41 with $R_{\text{rep}} = 1$, $1/2$ and $1/4$, which indicates the robustness at much higher user load compared with 5G-NR LDPC coded IDMA.

D. SIMULATION RESULTS

To verify the practical performance of enhanced IDMA with the new code family in random access, BLER simulations are carried out with the same parameters as those assumed for the BLER simulations of 5G-NR LDPC coded IDMA in Section IV-A. For the given user load λ, LDPC code rate R_{L}, and bit-repetition code rate R_{rep}, the practical individual outage probability of enhanced IDMA in random access can be obtained via BLER simulations, and the threshold at the given individual outage probability is denoted by SNR_{sim}. With ideal coded modulation assumed, the theoretical individual outage probability of enhanced IDMA based random access over Gaussian multiple access channel can also be calculated as described in Section IV-A, and the threshold at the given individual outage probability is referred to as the ideal threshold $\text{SNR}_{\text{ideal}}$ in the following discussion.

Firstly, we focus on the cases without bit-repetition code, i.e., $R_{\text{rep}} = 1$. For different user loads λ, the thresholds SNR_{sim} of enhanced IDMA with the new code family and 5G-NR LDPC code family are both obtained for comparison. Shannon limits are calculated for sum spectral efficiency equal to $\eta_{\text{s}}^{\text{avg}} = \lambda R_{\text{L}} R_{\text{rep}}$, and the gaps of SNR_{sim} at $p_{\text{out}} = 0.1$ to corresponding Shannon limit are shown in Fig. 12(a). Three different LDPC code rates $R_{\text{L}} = \{1/3, 1/4, 1/5\}$ are considered, and the corresponding single-user spectral efficiencies are $\eta_{\text{u}} = 0.33$, 0.25 and 0.20 bits/chip, respectively.

For 5G-NR LDPC coded IDMA with $R_{\text{L}} = 1/3$, the gap of SNR_{sim} at $p_{\text{out}} = 0.1$ to Shannon limit increases rapidly as the user load becomes higher than 1.6, which means it is difficult for 5G-NR LDPC coded IDMA to ensure

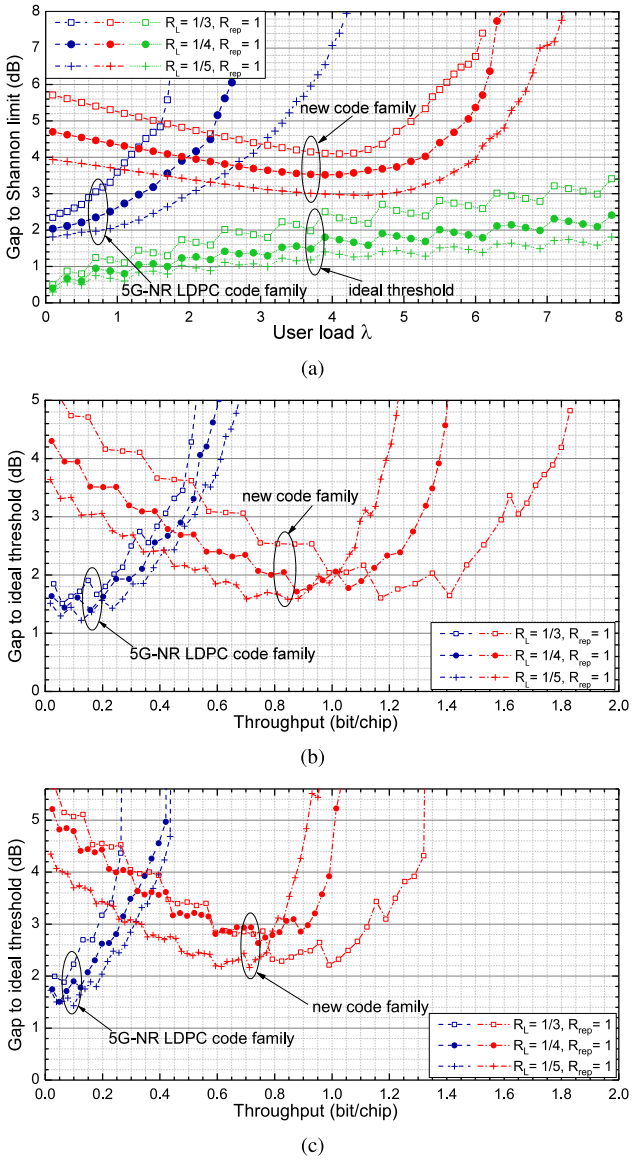

FIGURE 12. For enhanced IDMA with $R_L = \{1/3, 1/4, 1/5\}$ and $R_{rep} = 1$, (a) gap of practical threshold SNR_{sim} and ideal threshold SNR_{ideal} to Shannon limit vs. user load λ at $p_{out} = 0.1$, (b) gap of practical threshold SNR_{sim} to ideal threshold SNR_{ideal} vs. throughput $\mathcal{T}$ at $p_{out} = 0.1$, and (c) gap of practical threshold SNR_{sim} to ideal threshold SNR_{ideal} vs. throughput $\mathcal{T}$ at $p_{out} = 0.01$. SNR_{sim} and SNR_{ideal} are obtained by BLER simulations and theoretical outage analysis, respectively, in random access.

successful decoding of 90% of the transmitted messages with $\eta_u = 0.33$ bits/chip. By employing a lower-rate code in the 5G-NR LDPC code family, as in the cases of $R_L = 1/4$ and $R_L = 1/5$, the range of supported user load can be extended for 5G-NR LDPC coded IDMA. Furthermore, for all three cases of $R_L = \{1/3, 1/4, 1/5\}$, the performance of enhanced IDMA with the new code family is significantly improved at high user load, compared with that of 5G-NR LDPC coded IDMA.

The ideal thresholds SNR_{ideal} for different user loads are also obtained at $p_{out} = 0.1$, and the gaps of SNR_{ideal} to Shannon limit are shown in Fig. 12(a). To compare the performance of enhanced IDMA with different LDPC codes, the performance loss due to imperfect coding is evaluated through the gap of the practical threshold SNR_{sim}, obtained by BLER simulations, to the ideal threshold SNR_{ideal}, obtained by theoretical outage analysis with ideal coded modulation. Given $p_{out} = 0.1$, the system throughput of enhanced IDMA based random access can be calculated as $\mathcal{T} = \lambda\eta_u(1 - p_{out})$ for different user loads. The gaps of SNR_{sim} to SNR_{ideal} for different throughputs are demonstrated in Fig. 12(b), and the maximum gap of 4.00 dB is chosen for the following discussion.

For 5G-NR LDPC coded IDMA without bit-repetition code, though the range of supported user loads can be extended with lower-rate LDPC code, the maximum supported throughputs are still limited for all three code rates $R_L = \{1/3, 1/4, 1/5\}$. With the new code family, the performance of enhanced IDMA at relatively low throughput is even worse than that of the original 5G-NR LDPC code, since the target user number for code construction of these rates is $J_{target} = 18$. However, given the maximum gap of 4.00 dB, much higher throughput can be achieved with the new code family. For $R_L = 1/5$, the maximum supported throughput of enhanced IDMA is increased from 0.61 bits/chip, with 5G-NR LDPC code family, to 1.19 bits/chip, with the new code family. Meanwhile, by employing LDPC codes of higher rates, e.g., $R_L = 1/4$ and $1/3$, the maximum supported throughput for enhanced IDMA with the new code family can be further increased to 1.38 and 1.78 bits/chip, respectively, while those for 5G-NR LDPC code family are only 0.54 and 0.50 bits/chip. Moreover, the gaps between SNR_{sim} and SNR_{ideal} at $p_{out} = 0.01$ are also obtained and demonstrated in Fig. 12(c). Compared with those in Fig. 12(b), the gaps at $p_{out} = 0.01$ become larger, but the trends of curves are similar.

Then the LDPC code of $R_L = 1/4$ is taken as an example, and the effect of bit-repetition code is analyzed. For enhanced IDMA with $R_L = 1/4$ and $R_{rep} = \{1, 1/2, 1/4\}$, the gaps of SNR_{sim} to ideal threshold SNR_{ideal} at $p_{out} = 0.1$, corresponding to different user loads and different throughputs, are shown in Fig. 13(a) and (b), respectively. As we can see, for each bit-repetition code rate R_{rep}, the performance of enhanced IDMA with the new code family is significantly improved for high user load and high throughput, compared with that of 5G-NR LDPC coded IDMA.

In Fig. 13(a), with the practical threshold SNR_{sim} no more than 4.00 dB away from the ideal threshold, the maximum supported user loads of enhanced IDMA with the two code families can both be increased with the aid of bit-repetition code. For 5G-NR LDPC coded IDMA, the range of supported user load is 0–2.39 without bit-repetition code, and can be extended to 0–6.68 with $R_{rep} = 1/2$ and 0–16.40 with $R_{rep} = 1/4$. With the new code family, the maximum supported user load of enhanced IDMA can be further increased, and the ranges of supported user load are 0.22–6.11, 1.22–14.21 and 3.71–31.68 for $R_{rep} = 1$, $1/2$ and $1/4$, respectively.

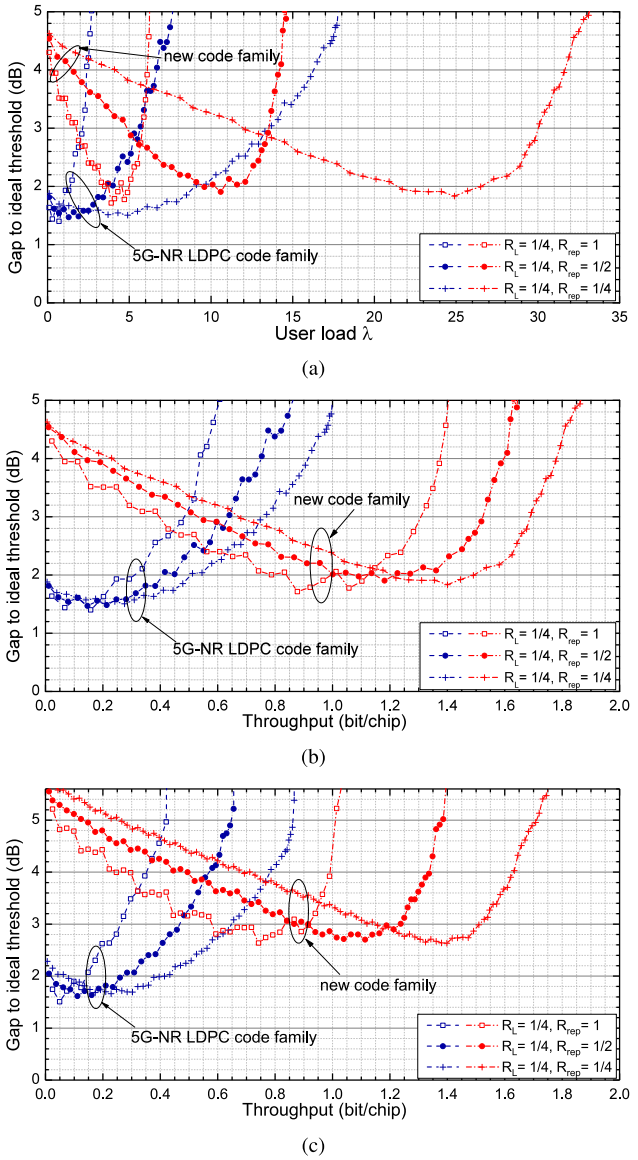

FIGURE 13. For enhanced IDMA with $R_{\mathrm{L}} = 1/4$ and $R_{\mathrm{rep}} = \{1, 1/2, 1/4\}$, (a) gap of practical threshold $\mathrm{SNR}_{\mathrm{sim}}$ to ideal threshold $\mathrm{SNR}_{\mathrm{ideal}}$ vs. user load λ at $p_{\mathrm{out}} = 0.1$, (b) gap of practical threshold $\mathrm{SNR}_{\mathrm{sim}}$ to ideal threshold $\mathrm{SNR}_{\mathrm{ideal}}$ vs. throughput $\mathcal{T}$ at $p_{\mathrm{out}} = 0.1$, and (c) gap of practical threshold $\mathrm{SNR}_{\mathrm{sim}}$ to ideal threshold $\mathrm{SNR}_{\mathrm{ideal}}$ vs. throughput $\mathcal{T}$ at $p_{\mathrm{out}} = 0.01$. $\mathrm{SNR}_{\mathrm{sim}}$ and $\mathrm{SNR}_{\mathrm{ideal}}$ are obtained by BLER simulations and theoretical outage analysis, respectively, in random access.

As shown in Fig. 13(b), the maximum supported throughputs for the two code families can also be increased with the aid of bit-repetition code. For example, the maximum supported throughput of enhanced IDMA with the new code family is 1.38 bits/chip for the case without bit-repetition code, and is increased to 1.60 and 1.78 bits/chip with $R_{\mathrm{rep}} = 1/2$ and $1/4$, respectively. At $p_{\mathrm{out}} = 0.01$, the gaps of $\mathrm{SNR}_{\mathrm{sim}}$ to ideal threshold $\mathrm{SNR}_{\mathrm{ideal}}$ for different throughputs are further given in Fig. 13(c), where similar trends can be observed. Note that, though the maximum supported user load and throughput can be increased by employing lower-rate bit-repetition code, the complexity of MUD also increases with more users accessing the same channel resources. Thus, a trade-off between the outage performance and the complexity of MUD could be made accordingly.

V. CONCLUSION

In this paper, enhanced IDMA is developed as a NOMA based random access solution by incorporating and designing rate-compatible RL-QC-LDPC codes into IDMA. 5G-NR LDPC codes can be directly employed for enhanced IDMA, which is capable of flexibly supporting various spectral efficiencies owing to the inherent rate compatibility. To improve the performance for high user load and system throughput, ECE algorithm is proposed to construct rate-compatible RL-QC-LDPC code families towards enhanced IDMA with moderate design complexity. With the edge-classification method EC-I, the number of candidate base matrices to be analyzed in each extension round is efficiently reduced, and with the edge-classification method EC-II, the diversity in the selected seed base matrices can be maintained for effective greedy search in further extension rounds. A new rate-compatible RL-QC-LDPC code family with fine code-rate granularity is constructed via ECE. For the scenarios with high user load and system throughput, the outage performance of enhanced IDMA based random access is shown significantly improved with the new code family. Moreover, the supported user load and system throughput can be further increased with the aid of bit-repetition code.

ACKNOWLEDGMENT

This paper was presented at the International Symposium on Turbo Codes & Iterative Information Processing (ISTC) 2018.

REFERENCES

[1] F. Boccardi, R. W. Heath, A. Lozano, T. L. Marzetta, and P. Popovski, "Five disruptive technology directions for 5G," *IEEE Commun. Mag.*, vol. 52, no. 2, pp. 74–80, Feb. 2014.

[2] *IMT Vision—Framework and Overall Objectives of the Future Development of IMT for 2020 and Beyond*, document ITU-R Recommendation M.2083, Sep. 2015.

[3] A. A. El Gamal and Y.-H. Kim, *Network Information Theory*. New York, NY, USA: Cambridge Univ. Press, 2011.

[4] H. S. Dhillon, H. C. Huang, H. Viswanathan, and R. A. Valenzuela, "Fundamentals of throughput maximization with random arrivals for M2M communications," *IEEE Trans. Commun.*, vol. 62, no. 11, pp. 4094–4109, Nov. 2014.

[5] L. Ping, L. Liu, K. Wu, and W. K. Leung, "Interleave division multiple-access," *IEEE Trans. Wireless Commun.*, vol. 5, no. 4, pp. 938–947, Apr. 2006.

[6] G. Song, X. Wang, and J. Cheng, "A low-complexity multiuser coding scheme with near-capacity performance," *IEEE Trans. Veh. Technol.*, vol. 66, no. 8, pp. 6775–6786, Aug. 2017.

[7] *Technical Specification Group Radio Access Network; NR; Multiplexing and channel coding (Release 15)*, document 3GPP TS 38.212 v2.0.0, Dec. 2017.

[8] T. J. Richardson and S. Kudekar, "Design of low-density parity check codes for 5G new radio," *IEEE Commun. Mag.*, vol. 56, no. 3, pp. 28–34, Mar. 2018.

[9] M. Beermann, F. Wickert, and P. Vary, "Highly flexible design of multi-rate multi-length quasi-cyclic LDPC codes," in *Proc. 8th Int. Symp. Turbo Codes Iterative Inf. Process. (ISTC)*, Bremen, Germany, Aug. 2014, pp. 37–41.

[10] *IEEE Standard for Local and Metropolitan Area Networks Part 16: Air Interface for Broadband Wireless Access Systems*, IEEE Standard 802.16e, May 2009.

[11] *Digital Video Broadcasting (DVB); Second Generation Framing Structure, Channel Coding and Modulation Systems for Broadcasting, Interactive Services, News Gathering and Other Broadband Satellite Applications (DVBS2)*, Standard ETSI EN 302 307, Mar. 2013.
[12] *Digital Video Broadcasting (DVB); Frame Structure Channel Coding and Modulation for a Second Generation Digital Terrestrial Television Broadcasting System (DVB-T2)*, Standard ETSI EN 302 755, Apr. 2012.
[13] *Digital Video Broadcasting (DVB); Next Generation Broadcasting System to Handheld, Physical Layer Specification (DVB-NGH)*, Standard ETSI EN 303 105, Jun. 2013.
[14] *Framing Structure, Channel Coding and Modulation for Digital Television Terrestrial Broadcasting System*, Chinese National Standard GB 20600-2006, Aug. 2006
[15] T. Richardson and R. Urbanke, "Multi-edge type LDPC codes," in *Proc. Workshop Honoring Prof. Bob McEliece 60th Birthday, California Inst. Technol.*, Pasadena, CA, USA, May 2002, pp. 24–25.
[16] *Low Density Parity Check Codes for Use in Near-Earth and Deep Space Applications*, document CCSDS 131.1-O-2, Orange Book, no. 2, Washington, DC, USA, Sep. 2007. [Online]. Available: https://public.ccsds.org/Pubs/131x1o1s.pdf
[17] D. Divsalar, S. Dolinar, C. R. Jones, and K. Andrews, "Capacity-approaching protograph codes," *IEEE J. Sel. Areas Commun.*, vol. 27, no. 6, pp. 876–888, Aug. 2009.
[18] T. V. Nguyen, A. Nosratinia, and D. Divsalar, "The design of rate-compatible protograph LDPC Codes," *IEEE Trans. Commun.*, vol. 60, no. 10, pp. 2841–2850, Oct. 2012.
[19] T. V. Nguyen and A. Nosratinia, "Rate-compatible short-length protograph LDPC codes," *IEEE Commun. Lett.*, vol. 17, no. 5, pp. 948–951, May 2013.
[20] T. Y. Chen, K. Vakilinia, D. Divsalar, and R. D. Wesel, "Protograph-based raptor-like LDPC codes," *IEEE Trans. Commun.*, vol. 63, no. 5, pp. 1522–1532, May 2015.
[21] Y. Zhang, K. Peng, Z. Chen, and J. Song, "Progressive matrix growth algorithm for constructing rate-compatible length-scalable raptor-like quasi-cyclic LDPC codes," *IEEE Trans. Broadcast.*, vol. 64, no. 4, pp. 816–829, Dec. 2018.
[22] Z. Si, R. Thobaben, and M. Skoglund, "Rate-compatible LDPC convolutional codes achieving the capacity of the BEC," *IEEE Trans. Inf. Theory*, vol. 58, no. 6, pp. 4021–4029, Jun. 2012.
[23] H. Zhou, D. G. M. Mitchell, N. Goertz, and D. J. Costello, Jr., "Robust rate-compatible punctured LDPC convolutional codes," *IEEE Trans. Commun.*, vol. 61, no. 11, pp. 4428–4439, Nov. 2013.
[24] L. Mu, Z. Liu, and Y. Fang, "Construction of time-invariant rate-compatible-low-density parity-check convolutional codes," *IET Commun.*, vol. 10, no. 9, pp. 1021–1026, 2016.
[25] D. G. M. Mitchell, M. Lentmaier, A. E. Pusane, and D. J. Costello, "Randomly punctured LDPC codes," *IEEE J. Sel. Areas Commun.*, vol. 34, no. 2, pp. 408–421, Feb. 2016.
[26] W. Hou, S. Lu, and J. Cheng, "Rate-compatible spatially coupled LDPC code ensembles based on repeat-accumulate extensions," *IET Commun.*, vol. 10, no. 17, pp. 2422–2426, Nov. 2016.
[27] Y. Zhang, K. Peng, and J. Song, "Enhanced IDMA with rate-compatible raptor-like quasi-cyclic LDPC code for 5G," in *Proc. IEEE Globecom Workshops (GC Wkshps)*, Singapore, Dec. 2017, pp. 1–6.
[28] Y. Zhang, K. Peng, X. Wang, and J. Song, "Performance analysis and code optimization of IDMA with 5G new radio LDPC code," *IEEE Commun. Lett.*, vol. 22, no. 8, pp. 1552–1555, Aug. 2018.
[29] J. Thorpe, *Low-Density Parity-Check (LDPC) Codes Constructed from Protographs*, document JPL IPN Progress Rep. 42-154, Aug. 2003.
[30] S. Myung, K. Yang, and Y. Kim, "Lifting methods for quasi-cyclic LDPC codes," *IEEE Commun. Lett.*, vol. 10, no. 6, pp. 489–491, Jun. 2006.
[31] K. J. Kim *et al.*, "Low-density parity-check codes for ATSC 3.0," *IEEE Trans. Broadcast.*, vol. 62, no. 1, pp. 189–196, Mar. 2016.
[32] S. I. Park, Y. Wu, H. M. Kim, N. Hur, and J. Kim, "Raptor-like rate compatible LDPC codes and their puncturing performance for the cloud transmission system," *IEEE Trans. Broadcast.*, vol. 60, no. 2, pp. 239–245, Jun. 2014.
[33] S. I. Park *et al.*, "Two dimensional code based on low density parity check and Reed–Solomon codes for the terrestrial cloud transmission system," *IEEE Trans. Broadcast.*, vol. 61, no. 1, pp. 75–83, Mar. 2015.
[34] L. Li, N. Jindal, and A. Goldsmith, "Outage capacities and optimal power allocation for fading multiple-access channels," *IEEE Trans. Inf. Theory*, vol. 51, no. 4, pp. 1326–1347, Apr. 2005.
[35] Y. Zhang, K. Peng, Z. Chen, and J. Song, "SIC vs. JD: Uplink NOMA techniques for M2M random access," in *Proc. IEEE Int. Conf. Commun. (ICC)*, Paris, France, May 2017, pp. 1–6.
[36] *Technical Specification Group Radio Access Network; Study on Non-Orthogonal Multiple Access (NOMA) for NR; (Release 16)*, document 3GPP TR 38.812 v0.2.0, Nov. 2018.
[37] *Tech. Specification Group Radio Access Network; Study Scenarios Requirements for Next Generation Access Technologies; (Release 15)*, 3GPP TR 38.913 v15.0.0, Jun. 2018.
[38] P. Popovski, K. F. Trillingsgaard, O. Simeone, and G. Durisi, "5G wireless network slicing for eMBB, URLLC, and mMTC: A communication-theoretic view," *IEEE Access*, vol. 6, pp. 55765–55779, 2018.
[39] T. Cheng, K. Peng, Z. Liu, and Z. Yang, "Efficient receiver architecture for LDPC coded BICM-ID system," *IEEE Commun. Lett.*, vol. 19, no. 7, pp. 1089–1092, Jul. 2015.

YUSHU ZHANG received the B.Eng. degree in electronic engineering from Tsinghua University, Beijing, China, in 2015, where she is currently pursuing the Ph.D. degree.

Her research area is wireless/mobile communication networks, and her current research interests include channel coding, coded modulation, non-orthogonal multiple access, and non-orthogonal multiple access-based random access.

KEWU PENG was born in Hefei, China. He received the B.Eng. degree in electronics engineering from the Hefei University of Technology, in 1993, the M.E. degree in electronics engineering from Tsinghua University, in 1996, and the Ph.D. degree in electrical engineering from the University of Minnesota, Minneapolis, in 2003.

He was a Researcher and a Lecturer with the Department of Electronic Engineering, Tsinghua University, from 1996 to 1999, where he has been with the Digital Television Research Center, as a Research Staff, since 2005, an Assistant Researcher, since 2006, and an Associate Professor, since 2009. He has published more than 90 journal and conference papers and holds more than 60 Chinese patents. His research interests include mobile/wireless communications, digital terrestrial/television broadcasting, and image/video transmission.

ZHANGMEI CHEN received the B.Eng. degree in electronic engineering from Tsinghua University, Beijing, China, in 2016, where she is currently pursuing the M.E. degree.

Her current research interests include wireless communication, channel coding, and coded modulation.

JIAN SONG (M'06–SM'10–F'16) received the B.Eng. and Ph.D. degrees in electrical engineering from Tsinghua University, Beijing, China, in 1990 and 1995, respectively.

He was with The Chinese University of Hong Kong and the University of Waterloo, Canada, in 1996 and 1997, respectively. He has been with Hughes Network Systems, USA, for seven years. He joined the Faculty Team as a Professor with Tsinghua University, in 2005, where he is currently the Director of DTV Technology R&D Center. He has been with quite different areas of fiber-optic, satellite, wireless, powerline, and visible light communications. He has published more than 200 peer-reviewed journal and conference papers. He holds two U.S. and more than 40 Chinese patents. His current research interest includes the area of digital TV broadcasting. He is a Fellow of IET.